Jurnal
Teknologi

Full Paper

HYDROGEN-RICH SYNGAS (HRS) PRODUCTION FROM RICE HUSKS WITH MIGRATORY PYROLYTIC FRONT METHOD IN TOP-LIT UPDRAFT GASIFIER (TLUD)

Abbas Fadhil[a]*, Mohd Fairus Mohd Yasin[a,b], Norazila Othman[c], Norikhwan Hamzah[a,b], Donghoon Shin[d], Hyunjin Lee[d], Muhammad Roslan Rahim[a]

[a]Faculty of Mechanical Engineering, Universiti Teknologi Malaysia 81310 UTM Johor Bahru, Johor, Malaysia
[b]High-Speed Reacting Flow Laboratory (HiREF), Universiti Teknologi Malaysia 81310 UTM Johor Bahru, Johor, Malaysia
[c]UTM Aeronautics laboratory, Universiti Teknologi Malaysia 81310 UTM Johor Bahru, Johor, Malaysia
[d]Department of Mechanical Engineering, Kookmin University, Seoul 02707, Korea

Article history
Received
7 September 2025
Received in revised form
11 December 2025
Accepted
11 December 2025
Published Online
29 August 2026

*Corresponding author
mohdfairus@mail.fkm.utm.my

Graphical abstract

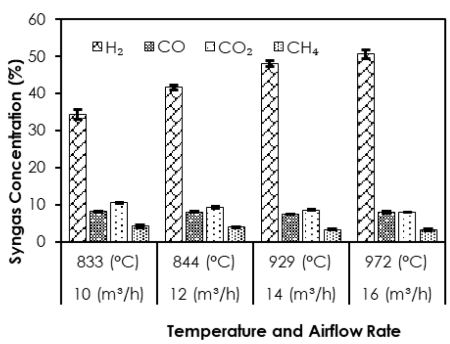

Abstract

Biomass gasification is an emerging method for hydrogen-rich syngas (HRS) production, though the systematic effects of gasification parameters on HRS composition remain unclear. Prior studies on top-lit-updraft gasifier (TLUD) focused on the effects of chamber configuration on syngas and char composition, with unclear insight into hydrogen enhancement processes in gasification. The present study examines the effects of airflow on HRS production in a TLUD reactor using rice husk pyrolysis. Flare flame that is formed at 10–16 m³/h air flow rate confirms the reactor reliability within specific conditions. Interestingly, H_2 concentration in the HRS rose linearly with air flow rate, reaching a maximum of 51% H_2 as the average reactor temperature increased above 900℃. CO_2 emission dropped by 25.7% at a high air flow rate due to high-temperature consumption by hot char in the reduction zone. Methane oxidation supplies water vapor in the oxidation zone, supporting the water-gas shift reaction to boost H_2 production. CO_2 emission of 0.15 kg/ kg H_2 shows that the present setup has a lower carbon footprint compared to that of the Steam Methane Reforming, though the energy requirement of 1325 MJ/kg shows that the gasification requires further optimization for field implementation.

Keywords: Hydrogen, top-lit updraft, gasification, syngas, rice husk

Abstrak

Pengegasan biojisim ialah kaedah yang baru muncul untuk pengeluaran syngas (HRS) kaya hidrogen, walaupun kesan sistematik parameter pengegasan pada komposisi HRS masih tidak jelas. Kajian terdahulu tentang pengegas draf terang atas (TLUD) memfokuskan pada kesan konfigurasi ruang pada syngas dan komposisi arang, dengan pandangan yang tidak jelas tentang proses peningkatan hidrogen dalam pengegasan. Kajian ini mengkaji kesan aliran udara ke atas pengeluaran HRS dalam reaktor TLUD menggunakan pirolisis sekam padi. Nyalaan nyalaan yang terbentuk pada kadar aliran udara 10–16 m³/j mengesahkan kebolehpercayaan reaktor dalam keadaan tertentu. Menariknya, kepekatan H_2 dalam HRS yang dihasilkan meningkat secara linear dengan kadar aliran udara, mencapai maksimum 51% H_2 apabila suhu reaktor purata meningkat melebihi 900℃. Pelepasan CO_2 menurun kepada 25.7% pada kadar aliran udara yang tinggi disebabkan penggunaan suhu tinggi oleh arang panas di zon pengurangan. Pengoksidaan metana membekalkan wap air dalam zon pengoksidaan, menyokong tindak balas anjakan air-gas untuk meningkatkan pengeluaran H_2. Pelepasan CO_2 sebanyak 0.15 kg/kg H_2 menunjukkan bahawa persediaan sekarang mempunyai jejak karbon yang lebih rendah berbanding dengan Steam Methane Reforming, walaupun keperluan tenaga sebanyak 1325 MJ/kg menunjukkan bahawa pengegasan memerlukan pengoptimuman lanjut untuk pelaksanaan medan.

Kata kunci: Hidrogen, aliran atas cahaya atas, pengegasan, syngas, sekam padi.

1.0 INTRODUCTION

Hydrogen is widely recognized as a clean-burning fuel, with growing global efforts to combat climate change highlighting its potential as a key future energy source. This interest stems from hydrogen's ability to support environmental sustainability due to its zero-emission characteristics [1, 2].

In recent decades, there has been a significant shift toward utilizing renewable biomass resources for the production of bioenergy and bio-products, driven by the need for sustainable energy solutions and reduced dependence on fossil fuels. Gasification has emerged as an efficient method for converting biomass into gaseous fuels, known for its simple design, ease of operation, and high energy conversion efficiency [3]. This process involves the thermal decomposition of solid biomass such as rice husks, which are favored due to their abundance, high volatile and carbon content, low cost, compatibility with TLUD systems, and environmental benefits under control conditions [4, 5].

Gasification methods used for hydrogen production such as downdraft, updraft, and top-lit updraft (TLUD) gasifiers differ in process efficiency, leading to variations in hydrogen yield and associated CO_2 emissions. Downdraft gasifiers generate CO_2 as a byproduct of biomass combustion [6], but their overall CO_2 emissions are typically lower than those from conventional fossil-fuel-based hydrogen production methods like steam methane reforming [7]. In contrast, updraft gasifiers generally operate at lower temperatures, which can reduce syngas quality and lead to incomplete combustion. This often results in higher emissions of particulate matter and unburned gases, contributing to increased CO_2 output [8]. TLUD gasifiers, however, offer improved syngas production efficiency compared to updraft systems due to their controlled combustion mechanism, allowing for cleaner syngas with reduced unburned residues.

TLUD gasifiers demonstrate greater syngas production efficiency than traditional updraft gasifiers, primarily due to their controlled combustion process. This enables the generation of cleaner syngas with fewer unburned particulates, potentially resulting in lower CO_2 emissions during hydrogen production [9]. Additionally, TLUD systems offer the combined benefits of hydrogen generation and biochar production, the latter of which can serve as a soil amendment or a long-term carbon sink. This supports carbon-negative energy strategies that aim not only to reduce emissions but also to capture and store atmospheric carbon. Beyond environmental advantages, TLUD gasifiers provide practical benefits in decentralized and rural energy applications. They require no external power supply or complex infrastructure, making them suitable for agricultural areas rich in biomass residues. The simplicity of the design and ease of operation allow for low-tech implementation. At the same time, the potential for modular scalability makes TLUD technology a promising solution for distributed hydrogen production in regions where centralized, fossil-based systems are impractical.

Previous studies have demonstrated that the TLUD gasification method holds considerable potential for efficient hydrogen (H_2) production. The work by James R *et al.* [9] found that when the airflow rate increased from 0.5 to 1.2 m^3/h, the temperature changed irregularly from 290 to 350^{o}C, and H_2 composition in syngas increased from 2.3 to 4.2% for rice husks using a top-lit updraft gasifier. This means that the hydrogen concentration may be low, but increasing the airflow will certainly increase the hydrogen concentration. Quintero-Coronel *et al.* [10] reported that in top-lit updraft gasification of palm kernel shell and coal, increasing the coal proportion and reducing coal particle size led to a product gas with higher energy content and concentrations of CO, CO_2, and H_2 at 9.5%, 13.5%, and 3%, respectively. Whereas, using rice husk, Kumar *et al*, [11] observed higher rate of gasification at 40% H_2, 12% CO, and 47% CO_2 due to high temperature and water gas shift reaction. James R. *et al*. [12] reported that the flaming pyrolysis is displaced from the top to the bottom of the gasifier as the reactions take place (migrating pyrolytic front). This gives the gasifier a characteristic configuration in which the combustion zone provides the needed heat for pyrolysis and reduction reactions to take place. The evaluated TLUD gasifier models exhibited particulate matter emissions significantly lower than those of conventional combustion equipment and within the thresholds established by legal regulations [13]. However, The TLUD gasification technique provides a flexible solution for biomass utilization. Recent studies have demonstrated that TLUD gasifiers possess the ability to produce substantial quantities of biochar in conjunction with syngas generation, establishing them as a dual-purpose system with enhanced value [9]. Additionally, the biochar in the TLUD reactor provides an advantage by partially degrading and combusting the volatile compounds generated during pyrolysis as they pass through it [14, 15].

Despite progress in down-lit updraft (DLUP) and TLUD systems, several aspects remain inadequately explored. Prior studies on TLUD focused on the effects of chamber configuration on syngas and char composition, with unclear insight into hydrogen enhancement processes in gasification. Despite TLUD's potential as a clean biomass combustion and gasification technology, the effect of airflow rate on flare flames remains unclear. Add to that its role in syngas generation remains underexplored compared to other gasifier types, such as updraft gasifiers or broader biomass gasification studies. Addressing this research gap could help optimize TLUD systems for enhanced syngas production, improving their efficiency and applicability in decentralized energy systems. Furthermore, hand, the relationship between gasification medium, including airflow, temperature, biomass type, and gasifier design, in the context of H_2 production necessitates additional research. Therefore, the present study investigates the use of a TLUD reactor for hydrogen-rich Syngas (HRS) Production via the pyrolysis and reduction of rice husk, thereby addressing an existing gap. Finally, this study enhances the understanding of updraft systems' operational dynamics, providing insights into the effects of gasification conditions on increasing H_2.

2.0 METHODOLOGY

2.1 Materials Preparation

The rice husk used in this experiment originated from Brilliant Supplies, Malaysia. The husk was obtained from local commercial rice varieties (primarily MR219), which belong to the species Oryza sativa L. It is placed in plastic bags to prevent moisture. The properties of the used rice husk are determined by proximate and ultimate analysis according to ASTM D5142 and ASTM D3176, respectively, as shown in Table 1.

The ultimate analysis of rice husk as described suggests a promising potential for its use as a feedstock in TLUD/G. Based on the composition of carbon, hydrogen, oxygen, nitrogen, and sulfur the relatively high contents of carbon (38.6%) and hydrogen (5.5%) are critical because these elements are primary contributors to heat generation during combustion. Carbon and hydrogen combine with oxygen during burning to release energy, making the substance highly combustible and efficient as a fuel source. There is a slight difference between previous studies and the current study, where for rice husk gasification a study by [16] with a carbon content value of 38.47%. Another study by [17] showed that the value of carbon content was 37.54%. The variation might be due to differences in the geographical origin of the rice husk, its cultivation conditions, or specific characteristics of the rice variety used. On the other hand, oxygen content at 54.1% also plays a role in the combustion process, although its high presence is typical in organic materials like rice husk. Oxygen within the biomass can lead to a more complete and efficient combustion process, reducing the reliance on external oxygen sources and potentially lowering the emissions of unburnt hydrocarbons. In the same context, the low levels of nitrogen (0.8%) and sulfur (1.0%) are particularly advantageous from an environmental standpoint. The combustion of materials containing high nitrogen and sulfur often leads to the formation of nitrogen oxides (NOx) and sulfur oxides (SOx), which are significant pollutants that contribute to acid rain, smog, and respiratory problems in humans. The low quantities in rice husk suggest that its combustion would result in minimal emissions of these harmful gases, aligning with environmental protection standards.

In addition, the proximate analysis showed approximately 6% of moisture contents and it is lower than the reading by [18] predicted as 10.59%. In this study, the confirmation of the moisture contents is important to avoid the incomplete combustion phenomenon, it happens if high moisture content levels for feedstock were used [19]. According to the [20] study, which analyzed Elaeis guineensis leaves, the level of moisture content was 18.8%. Another study by Maliki *et al*. [21] utilized corn cob; the moisture content was 17.38%. On the other hand, biomass with highly volatile matter is particularly valuable for processes such as gasification and pyrolysis, where it can enhance the yield and quality of the produced syngas [22]. The volatile matter values observed in this study (73%) were generally higher when compared to previous studies. For instance, a study by Steven et al. [23] noted volatile matter levels in rice husk were 58.13%. Different results were obtained from different feedstocks. Kabir Ahmad *et al.* [24] reported that the gasification values are 70.82% using coconut shell (CS), with the variation likely resulting from differences in the content of volatile compounds (excluding water) present in the biomass and binders. In terms of ash content, the rice husk used in this study exhibited a value of 12%, which is consistent with the range of 12.81% to 17.51% reported by Ríos-Badrán *et al.* [25]. Such variation is commonly attributed to differences in rice husk sources, harvesting conditions, or analytical techniques. Furthermore, the rice husk sample demonstrated a fixed carbon content of 9%, placing it within the expected range based on comparable findings in previous studies. This implies that the results are consistent enough to validate the utility of rice husk as a biomass resource.

Table 1 Proximate and ultimate analysis of rice husk

Ultimate analysis	**Value (wt%)**
Nitrogen (N)	0.8
Carbon (C)	38.6
Hydrogen (H)	5.5
Sulfur (S)	1.0
Oxygen (O)	54.1
Proximate analysis	
Ash	12
Volatile matter	73
Fixed carbona	9
Moisture	6

2.2 Experiment First Setup

The schematic diagram of the TLUD system is shown in Figure 1. The system consists of the reactor and the chamber, made of mild steel, in addition to the air blower and gas production tube. The main equipment of the rice husk gasification was designed to treat 3.5 kg of dried rice husk per batch. A Stanley variable-speed blower (model STPT600, 1600 rpm) was used to supply adjustable airflow rates. The airflow rate is controlled through a valve connected to a transparent high-pressure air flow meter with a maximum capacity of 50 m³/h was used to measure and adjust the airflow. The typical accuracy for this type of meter is about ±3% of full scale, which corresponds to ±1.5 m³/h at the 50 m³/h range. Since the airflow rates in this study (10–16 m³/h) are well below the meter's maximum range, the measurement error is minimal and does not affect the experimental results. The chamber joint is connected axially to the multi-hole plate and from there to the reactor to determine the required airflow rate. The airflow rate of the developed system is from 10 to 16 m3/h with a 2 m3/h increment. To compare temperature and airflow rate, three peak temperature points were measured in the oxidation zone using a thermocouple type K. The temperature starts to be measured by the pico log program contacting the thermocouple at time zero. After 3 min, the T1 will reach the peak, and the pyrolysis process begins. The three temperatures were measured within 24 minutes. They were determined every 20 cm, starting from the top cover of the reactor to the bottom of the reactor, and named T1, T2, and T3, as seen in Figure 2.

All measurements in this experiment used calibrated instrumentation to provide the most reliable data for analysis. The TLUD Gasifier provides consistent operational parameters; the temperature was monitored through thermocouples with an accuracy of ±1-2 degrees Celsius (°C) (this may vary depending on the type of thermocouple used). The mass of rice husks placed into the gasifier was measured utilizing an electronic scale capable of reading to the nearest gram (1g) and with an accurate range of ±0.5-1% of the total measuring capacity. This allows for precise measurement of feedstock input. The composition of the syngas was determined using a gas chromatograph (GC), which has an analytical accuracy of ±0.1-0.5% for the major components H_2, CO, CO_2, and CH_4. To further reduce analytical variability, the GC was calibrated with known, certified standard gas mixtures before taking any samples. Therefore, based on these levels of accuracy, it can be inferred that all calculated parameters associated with this experiment (i.e., carbon conversion efficiency, syngas composition, and lower heating value) can be reliably derived from repeatable measurements.

The operational process of the TLUD gasifier involved loading the reactor with rice husks, followed by ignition of the topmost biomass layer. Once ignited, the reactor was closed and allowed to stabilize for a few minutes. The initial combustion provided the thermal energy necessary to initiate pyrolysis. Controlled airflow was then introduced from the bottom of the reactor. As the pyrolysis front progressed downward, it produced syngas and left behind the biochar in the upper section. The heat generated from partial oxidation at the combustion zone sustained the pyrolysis reactions, enabling continuous operation without the need for external heating.

Generally, the thermochemical conversion of biomass with the migratory pyrolysis method encompasses several interrelated processes, as shown in Figure 2. The initial stage (starting from the bottom of the reactor) is referred to as drying, as shown in Equation (1). At this stage, the process of evaporation of water from the biomass at low temperatures can be easily achieved [14]. The second stage is called the migrating pyrolytic front phase (MPF). It rests on the top of the unburnt feedstock and goes down through it, moving opposite to the gases that are released [14]. The pyrolysis of fuel generates volatile gases such as CO, CH_4, CO_2, H_2, and hydrocarbons or tars, leaving behind char [9, 26, 27], as presented in Equation (R2). In the third stage, the partial oxidation phase of these volatiles and char releases additional heat that is required for pyrolysis and reduction reactions to occur. The O_2 concentration starts from the bottom of the reactor in large quantities and gradually decreases until it reaches the top of the reactor. This amount of O_2 is sufficient to continue partial combustion at the top even though there is no additional airflow from the top. Moreover, the incomplete combustion of tars takes place that resulting in CO and H_2 [12]. CH_4 can also react with oxygen in the oxidation zone of the TLUD gas generator, especially at high air flow rates where more O_2 is available to support water gas-shift in the reduction zone [11], as shown in Equations (R3) through (R8). Finally, reduction is therefore the final step of thermochemical conversion[26], as presented in Equations (R9) through (R14). The solid residue from the preceding stage of pyrolytic decomposition is transported into the gas phase, resulting in flammable gases. When CO_2 and H_2O pass over heated char, they are converted to CO, H_2, and small-chain hydrocarbons (producer gas), resulting in clean combustion [14, 27]. Although the reaction rates for CO and CO_2 formation exhibit a slight increase, the extent of this rise is insufficient to influence their concentrations in the generated syngas significantly. CO and CO_2 are produced through certain reactions, but at the same time are consumed through other reactions [28]. In addition, the steam reforming reactions of tar occur and lead to the production of more CO and H_2 [29]. Consequently, the TLUD gasifier provides the benefit that the tar generated during pyrolysis is partly degraded and combusted as it traverses the heated char layer above [15, 30]. On the other hand, the equivalence ratio (ER) results were 0.27, 0.32, 0.38, and 0.43 at airflow rates of 10 to 16 (m^3/h), respectively.

Drying:

$$Biomass + Heat \rightarrow Dry\ Biomass + H_2O \quad \text{(R1)}$$

Pyrolysis:

$$Dry\ Biomass + Heat \rightarrow C + Tar + Volatile\ gases\ (CO + H_2 + CH_4 + CO_2) \quad \text{(R2)}$$

Partial Oxidation:

$$CO + \frac{1}{2}O_2 \rightarrow CO_2 \quad \text{(R3)}$$

$$H_2 + \frac{1}{2}O_2 \rightarrow H_2O \quad \text{(R4)}$$

$$C + \frac{1}{2}O_2 \rightarrow CO \quad \text{(R5)}$$

$$C + O_2 \rightarrow CO_2 \quad \text{(R6)}$$

$$CH_4 + 2O_2 \rightarrow CO_2 + H_2O \quad \text{(R7)}$$

$$Tar + \frac{1}{2}O_2 \rightarrow CO + H_2 \quad \text{(R8)}$$

Reduction:

$$C + H_2O \rightarrow CO + H_2 \quad \text{(R9)}$$

$$C + 2H_2 \rightarrow CH_4 \quad \text{(R10)}$$

$$C + CO_2 \rightarrow 2CO \quad \text{(R11)}$$

$$CO + H_2O \rightarrow CO_2 + H_2 \quad \text{(R12)}$$

$$Tar + H_2O \rightarrow CO + H_2 \quad \text{(R13)}$$

$$CH_4 + H_2O \rightarrow CO + 3H_2 \quad \text{(R14)}$$

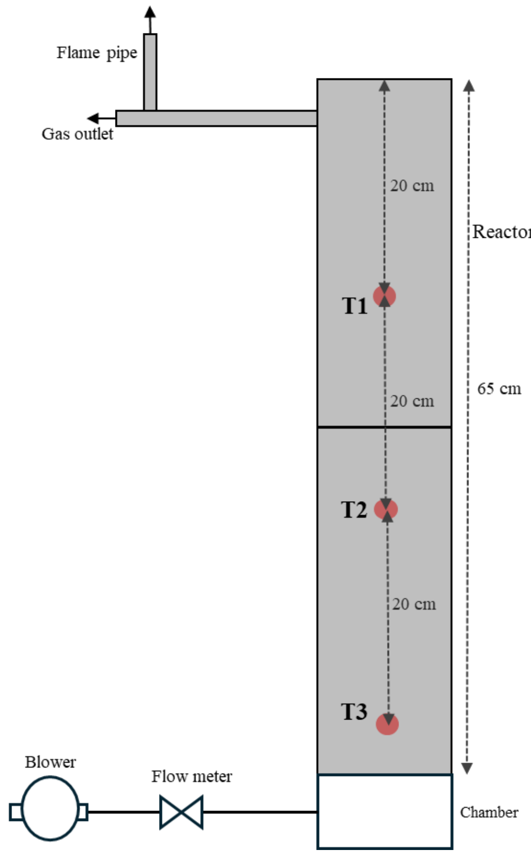

Figure 1 Top lit updraft gasifier system and temperature measuring locations schematic diagram

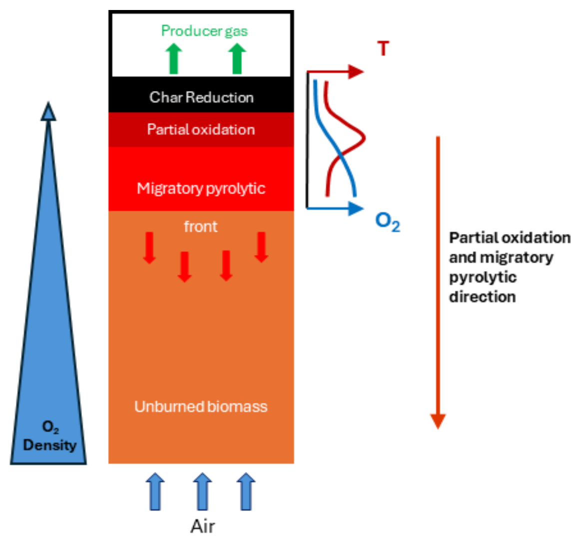

Figure 2 Pyrolysis front moving from top to bottom; chemical reactions occurring as the front progresses towards unburned biomass

3.0 RESULTS AND DISCUSSION

3.1 Flare Flame Observation and Transient Temperature Distribution

Flare flame types are compatible with varying amounts of airflow, which affects the flare flame color. Suitable flare flames were obtained at airflow rates of 10 to 16 m³/h. Figure 3 shows the flare flame at an airflow rate of 16 m³/h and an approximate flare flame volume of 608 cm³, with 30Cm long. Air movement affected the resulting flare flame, which was good. Flare flames could be obtained after 5 minutes of gasification system operation, and the flare flame speed increased with increasing airflow. This may be related to the color change.

Figure 3 Flare flame observation for 16 m³/h airflow rate

The reactor consists of two parts connected by a flange that divides the upper and lower parts, as shown in the left image of Figure 4.

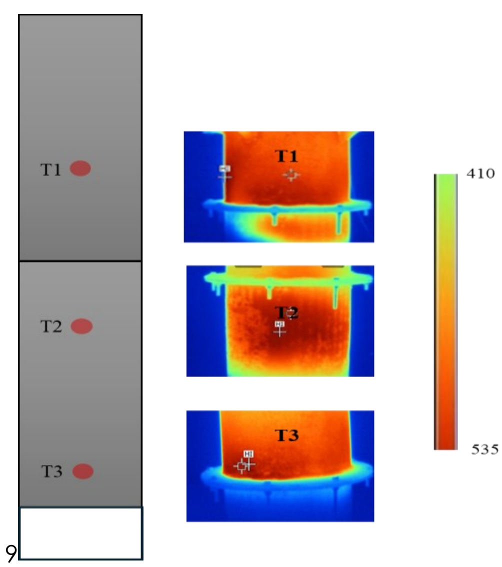

Figure 4 region using temperature scanner

The temperature starts from the upper part of the gasifier. According to the first picture, T1 is measured in the first part. Then it moves to the bottom of the flange and T2 is measured, at the top of the second part. Finally, it goes to the bottom of the second part near the axle plate where T3 is measured. The temperature transfer from the top to the bottom occurs due to the downward movement of the migrating pyrolytic front.

The gasification process took a total of 24 min. For T1, the temperature was measured after around 8 min, and after the oxidation layer reached T2, the second temperature was measured after around 8 min (16 min from the process starting). Finally, T3 was measured after the last 8 min (24 min from the process starting).

The effect of the reactor temperature in the oxidation zone was studied depending on the difference in airflow rate. The average temperature of the chamber ranges from about 833°C to 972°C, as indicated in Figure 5.

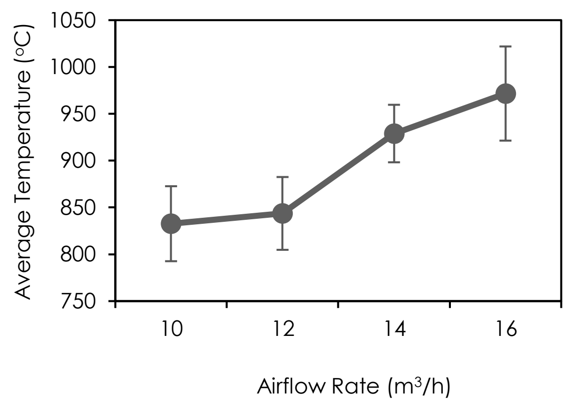

Figure 5 Effect airflow rate on the average temperature in TLUD

The present study demonstrates that there is a linear correlation between the rate of airflow and the average temperature, which indicates that the temperature rises in tandem with the increase in the airflow rate due to the conductive effect within the chamber wall. As can be seen in Figure 6, the maximum temperature is fairly stable, with a few increases at the bottom, as it moves with the oxidation zone from top to bottom at a fixed airflow rate. These exothermic reactions release significant amounts of heat. This heat is radiated downward, increasing the temperature of the gases and particles as they move toward the bottom. On the other hand, it appears that the airflow rate is a major predictor of temperature within the range that was measured. This may be because higher airflows allow for more efficient energy transfer [9]. In other words, an increased airflow rate means more oxygen is available. More oxygen promotes faster combustion of char and volatile gases (produced by rice husk pyrolysis), which generates heat. The generated heat leads to an increase in temperature in the gasifier. Higher temperatures improve pyrolysis and gasification efficiency and facilitate more complete combustion of volatile gases. This result is similar to a study by [31], which indicated that the positive relationship

The relationship between airflow rate and temperature arises from the intrinsic correlations of velocity, pressure, and temperature, as changes in these factors propagate rapidly through the medium. As shown in this plot of the relationship between airflow rate and temperature, the temperature has increased significantly. This is due to the increased airflow, which facilitates faster heat diffusion, leading to an increased hydrogen content. Taking all factors into account, the airflow rate appears to be a reliable indicator of temperature within the measured range.

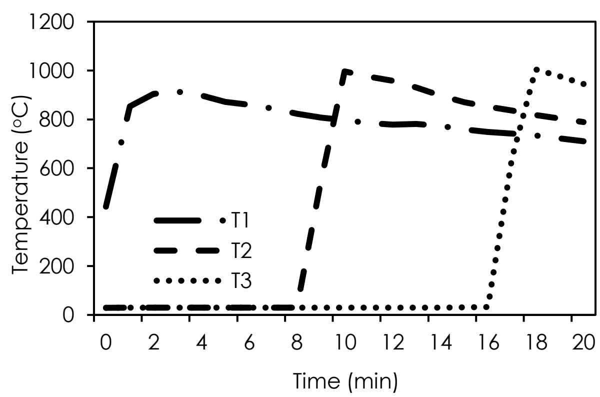

Figure 6 The temperature for T1, T2, and T3 at airflow rate 16 m³/h

3.2 Effect Airflow Rate on the Syngas Concentration

Figure 7 (a) shows the effects of airflow rate on the percentage of H_2 where the H_2 concentration increases with airflow rate. The lowest H_2 concentration occurs at 10 m³/h air flow rate, suggesting that this flow rate might result in conditions less favorable for hydrogen generation. The rate of change in hydrogen production is higher at low air flow rates compared to that of the high air flow rates. The highest H_2 percentage reached approximately 51% at an airflow rate of 16 m³/h. That is interestingly among the highest reported in literature to the best of the author's knowledge. A previous study has reported 48.7 % of H_2 production with the increased equivalence ratio [32]. This study also used rice husks, and the high temperatures and use of air and steam were effective in stimulating the reaction of water gas shift the produced syngas contains a higher proportion of H_2. The primary reaction to produce H_2 is pyrolysis, which happens within the pyrolytic region [33]. The air flow increases the temperature in the pyrolysis zone, which enhances pyrolysis and leads to the production of more volatile gases, which are later converted into hydrogen. Then, the partial oxidation of the tar in the oxidation zone, as shown in equation (R8), leads to the production of more H_2. in addition, the steam reforming reactions of tar in the reduction zone occur as shown in equation (R13) and lead to the production of more CO and H_2 [29, 34]. Moreover, reduction reactions in TLUD occur when CO_2 and H_2O react with char (the solid carbon residue left from biomass) to form CO and H_2. The main agent in the oxidation zone is oxygen, as shown in equations from (R3 to R8). The increase in O_2 in the oxidation zone produces large quantity of water, which supports the reduction reactions in the reduction zone, as shown in equations from (R9 to R14). Therefore, when sufficient O_2 is present, the system's ability to maintain the right conditions for these reduction reactions improves, leading to more hydrogen formation. Similarly, Dmitrenko *et al*. [35] indicated that improving H_2 production efficiency relies heavily on optimizing the airflow rate.

Figure 7 (b) shows the relationship between airflow rate and CO%. At all airflow rates, CO levels are relatively stable. Like H_2 production, the pyrolysis, partial oxidation of the tar, reduction reactions when CO_2 and H_2O react with char, and steam reforming reactions of tar lead to the production of CO as shown in equations (R5, R8, R9, R11, R13, and R14). Furthermore, the partial oxidation of the char also increases CO in the syngas. More oxygen helps sustain the conditions in the reduction zone by providing enough heat from the oxidation zone, which supports the conversion of CO_2 into CO and enhances the overall CO production in the gasifier. In other words, when O_2 is available, the conversion of char into gaseous components is enhanced because hot char serves as a reaction surface to reduce CO_2 into CO. These results were compatible with previous studies [36] [37] [38]. Especially in TLUD, carbon monoxide is often produced and consumed simultaneously and in overlapping areas. CO production reaction as shown in equations (R5, R9, and R11) while CO consumption reaction is shown in equations (R3 and R12).

Figure 7(c) shows how the CO_2 content changes with different air flow rates). From 10 to 14 m³/h, CO_2 levels are relatively high. At 16 m³/h, CO_2 levels drop to their lowest value. At low air flow rates, a limited amount of O_2 will be available for oxidation reactions, leading to partial oxidation as shown in Equation (R5). CO is then oxidized to CO_2 as shown in Equation (R3), reducing the heating required for the reduction reactions and causing low gasification efficiency. This results in an increase in CO_2 in the reduction zone, resulting from the water-gas shift reaction as shown in Equation (R12), at a temperature of 150 - 300 °C [39]. Conversely, when air flow increases, the system tends to provide more oxygen for the oxidation reactions in the oxidation zone, as shown in Equation (R6). Consequently, carbon monoxide oxidation will occur, and carbon dioxide will decrease by around 25.7%. This will increase the temperature in the oxidation zone due to the higher air flow rate and enhance gasification efficiency in the reduction zone. This activates the reverse conversion of water and gas to reduce carbon dioxide and increase hydrogen, as shown in the reverse equation (R12), at temperatures of 300-500°C [39]. Thus, the increase in air flow changes the balance of reactions in the gasifier. However, due to the char, carbon dioxide is absorbed by the biomass as solid carbon [40].

From Figure 7(d), the results show that the methane content decreased at different air flow rates. The higher the air flow rate, the lower the methane content. At low air flow rates, the temperature is low, the pyrolysis is incomplete, and the reforming process is poor. The reaction that occurs at low air flow rates is an Increase of methane and tar and a decrease of other volatile gases, as shown in equation (R2). Typically, at high air flow rates, CH_4 decreases due to reaction with oxygen in the oxidation zone to convert to CO_2 and H_2O as shown in equation (R7). Thus, the oxidation of methane decreased methane, and the water increased to enhance the reactions in the reduction zone, as shown in equations (R9, R12, R13, and R14). The reactions that occurred between methane and air flow rates indicate that increasing air flow rates increases hydrogen production and decreases methane production at high temperatures. High temperatures decompose methane into hydrogen and solid carbon (soot or char).

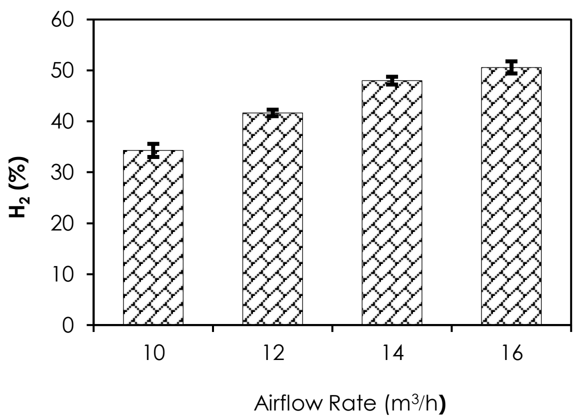

(a)

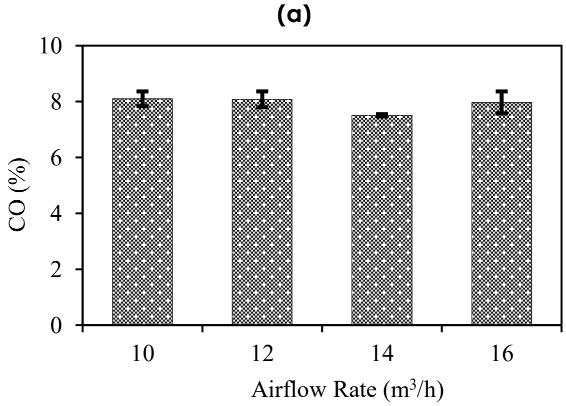

(b)

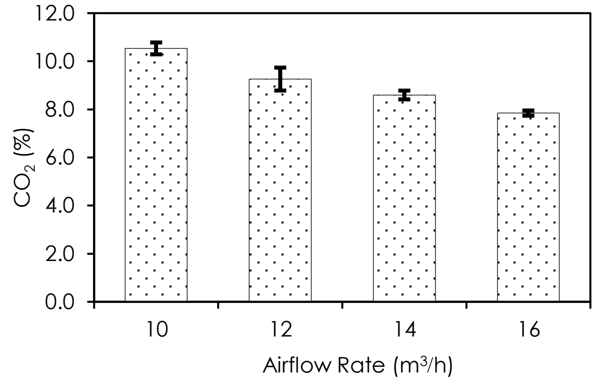

(c)

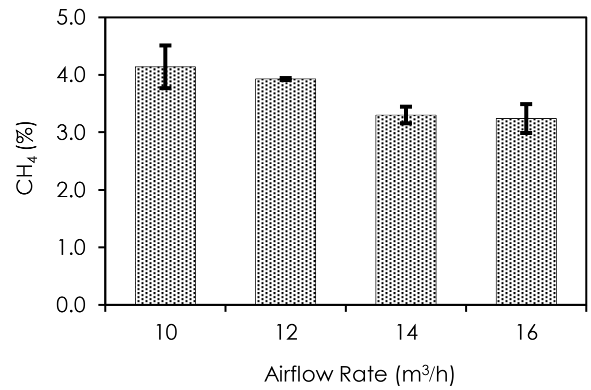

(d)

Figure 7 Effect airflow rate on: (a) H_2 concentration, (b) CO concentration, (c) CO_2 concentration, and (d) CH_4 concentration

Figure 8. shows the composition of syngas (H_2, CO, CO_2, and CH_4) at average temperatures from 833°C to 971°C. A significant increase in hydrogen concentration is observed, reaching approximately 51%. This increase in H_2 can be attributed to the improved steam reforming process, as shown in Equation (R14), and the water-gas shift reactions, as shown in Equation (R12), both of which are favored at higher temperatures. Meanwhile, the CO_2 concentration decreases slightly, indicating that it is partially consumed in the water-gas shift reaction at higher temperatures. Interestingly, CO_2 levels decrease more significantly despite being a product of the shift reaction; this can be explained by the Boudoir reaction, as shown in Equation (R11), in which CO_2 reacts with hot char, and possibly with other CO_2-consuming reactions involving tar or hydrocarbons at high temperatures. The CH_4 content also decreases, most likely due to thermal cracking and formation at higher temperatures. This suggests a strong correlation between gas composition and average temperature.

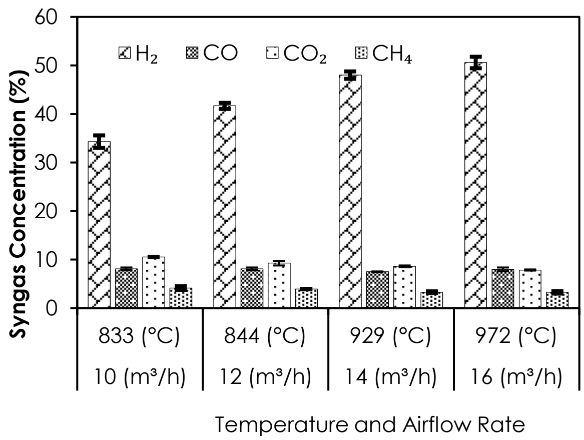

Figure 8 The relationship syngas concentration and Temperature

3.3 The Techno-environmental Analysis of HRS Production

Figure 9 presents the relationship between energy input and CO_2 emission per unit mass of H_2 produced from rice husk gasification in a TLUD reactor at varying airflow rates. The calculated values demonstrate that, at an airflow rate of 10 m³/h, the energy requirement reaches approximately 1988 MJ per kg of H_2 produced, while the corresponding CO_2 emission per unit H_2 is around 0.31 kg. As the airflow rate increases (16 m³/h), both energy input per kg of H_2 (1325 MJ) and CO_2 emission decrease (0.15 kg), indicating an improvement in H_2 production efficiency and carbon performance. With the continuous increase in hydrogen and the decrease in carbon dioxide, the carbon monoxide remaining almost constant, the combustion efficiency will decrease. The lost energy is due to heat, char, and other gases CO, CO_2, and CH_4. The excess energy input leads to a decrease in combustion efficiency. Combustion efficiency is the ratio of usable energy output to total energy input. However, the increase in hydrogen is a reaction resulting from pyrolysis, reduction, and not oxidation. However, when benchmarked against established industrial-scale H_2 production technologies, this process displays both opportunities and limitations. This difference arises from several fundamental processes and design limitations, such as (Small-Scale, Non-Integrated Operation, Low Hydrogen Yield from Biomass, High Unutilized Energy Losses, and Lack of Process Intensification. Conventional H_2 production methods such as Steam Methane Reforming (SMR) typically require between 142–190 MJ/kg H_2, depending on process integration and heat recovery strategies. However, SMR emits approximately 9–12 kg of CO_2 per kg of H_2 produced [7], making it a major contributor to industrial greenhouse gas emissions despite its economic viability. Therefore, when comparing the CO_2 emission intensities, the TLUD reactor method using rice husks demonstrates a substantially lower carbon footprint compared to that of the Steam Methane Reforming which is about 0.15 kg CO_2/kg H_2, making it a more sustainable option in terms of greenhouse gas emissions. In summary, while the current hydrogen output and energy efficiency of the TLUD method are lower compared to mature industrial processes, the environmental advantages, low feedstock cost, and co-benefits of biochar production underscore its sustainability potential. The findings from Figure 9 reinforce the necessity for continued development of the TLUD method, particularly in improving hydrogen concentration in syngas, enhancing heat management, and integrating char utilization systems. With targeted advancements, TLUD gasifiers could offer a viable alternative or supplement to traditional hydrogen production methods in future green energy portfolios.

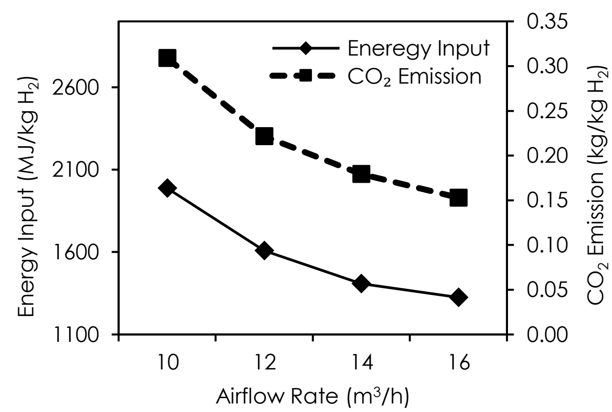

Figure 9 Energy input and CO_2 with variation of airflow rate

4.0 CONCLUSION

This study investigated the application of a TLUD reactor to produce HRS from rice husk gasification. where the reduction reactions reduce the carbon monoxide and carbon dioxide. Emphasis was placed on the effect of air flow rates on the HRS production. Although flare flame characteristics are examined as part of our observations, flare flame stability is not the primary aim of this study and is therefore discussed only insofar as it influences the overall gasification performance. The steam generated by methane oxidation, in turn, supports the water-gas shift reaction in the reduction zone to increase hydrogen content where the H_2 concentration increases with airflow rate. At 16 m³/h, the hydrogen concentration reached its maximum at approximately 51 %, and the carbon dioxide concentration was the lowest at 7.8%. The average temperature was 972°C at a flow rate of 16 m³/h. A significant correlation was observed between temperature and the concentrations of carbon monoxide, carbon dioxide, methane, and hydrogen that were produced. The concentrations of hydrogen, carbon monoxide, methane, and carbon dioxide were 51%, 8%, 3.2%, and 7.8%, respectively with remaining gas component consists of N_2. The results indicate that the H_2 production efficiency is related to the flame temperature, necessitating increased airflow rates to achieve optimal results. This is because partial oxidation reactions release the heat required for pyrolysis and reduction reactions. The synergistic effects of MPF result in high hydrogen production and low CO_2 emissions from its reduction with hot char. Therefore, compared to the intensity of CO_2 emissions, the TLUD reactor method using rice husks exhibits a significantly lower carbon footprint compared to that of the Steam Methane Reforming, at only 0.15 kg CO_2/kg hydrogen, making it a more sustainable option in terms of greenhouse gas emissions. The research highlights the importance of regulating airflow rates to enhance hydrogen production from rice husk pyrolysis and reducing emissions.

Conflicts of Interest

The authors declare that there is no conflict of interest regarding the publication of this paper.

Acknowledgement

The authors would also like to thank the Research Management Center and Faculty of Mechanical Engineering, Universiti Teknologi Malaysia for the knowledge transfer and providing the research facilities and space to undertake this research study.

References

[1] Hoang, A. T., *et al.* 2023. Hydrogen Production by Water Splitting with Support of Metal- and Carbon-Based Photocatalysts. *ACS Sustainable Chemistry & Engineering*. 11(4): 1221–52. https://doi.org/10.1021/acssuschemeng.2c05226.

[2] Nguyen-Thi, T. X., and T. M. T. Bui. 2023. Effects of Injection Strategies on Mixture Formation and Combustion in a Spark-Ignition Engine Fueled with Syngas–Biogas–Hydrogen. *International Journal of Renewable Energy Development*. 12(1): 118–28.

[3] Vidian, F., A. Situmeang, H. Fitriani, T. Arief, and M. Saleh. 2024. Experimental Biomass Gasification in Updraft Gasifier with Gas Outlet at Reduction Zone and Air Supply Using Suction Blower. *Journal of Advanced Research in Fluid Mechanics and Thermal Sciences*. 118(1): 155–62. https://doi.org/10.37934/arfmts.118.1.155162.

[4] Le Tan, N. T., N. P. Thien Le, T. P. Vo, T. P. Mai, and D. Q. Nguyen. 2022. Experiment and Simulation of Rice Husk Gasification Process with a Downdraft Gasifier. *Chemical Engineering Transactions*. 97: 79–84. https://doi.org/10.3303/CET2297014.

[5] Simanjuntak, J. P., K. A. Al-Attab, E. Daryanto, B. H. Tambunan, and Eswanto. 2022. Bioenergy as an Alternative Energy Source: Progress and Development to Meet the Energy Mix in Indonesia. *Journal of Advanced Research in Fluid Mechanics and Thermal Sciences*. 97(1): 85–104. https://doi.org/10.37934/arfmts.97.1.85104.

[6] Ali, A. M., *et al.* 2022. Process Optimization and Economic Evaluation of Air Gasification of Saudi Arabian Date Palm Fronds for H_2-Rich Syngas Using Response Surface Methodology. *Fuel*. 316: 123359. https://doi.org/10.1016/j.fuel.2022.123359.

[7] Younus, T., A. Anwer, Z. Asim, and M. S. Surahio. 2018. Production of Hydrogen by Steam Methane Reformation Process. *E3S Web of Conferences*. 51: 03003. https://doi.org/10.1051/e3sconf/20185103003.

[8] Yousef, S., J. Eimontas, K. Zakarauskas, and N. Striūgas. 2025. Oxygen Updraft Gasification of Euro Cotton Banknotes Waste for Hydrogen-Rich Syngas Production. *Journal of the Energy Institute*. 118: 101906. https://doi.org/10.1016/j.joei.2024.101906.

[9] James R., A. M., W. Yuan, M. D. Boyette, and D. Wang. 2018. Airflow and Insulation Effects on Simultaneous Syngas and Biochar Production in a Top-Lit Updraft Biomass Gasifier. *Renewable Energy*. 117: 116–24. https://doi.org/10.1016/j.renene.2017.10.034.

[10] Quintero-Coronel, D. A., Y. A. Lenis-Rodas, L. A. Corredor, P. Perreault, and A. Gonzalez-Quiroga. 2021. Thermochemical Conversion of Coal and Biomass Blends in a Top-Lit Updraft Fixed-Bed Reactor: Experimental Assessment of the Ignition Front Propagation Velocity. *Energy*. 220: 119702. https://doi.org/10.1016/j.energy.2020.119702.

[11] Kumar, A., D. S. Pandey, and T. Mondal. 2025. Experimental Investigation of Process Parameters for Hydrogen-Rich Syngas Production from Rice Husk Gasification. *Sustainable Chemistry for Climate Action*. 6: 100061. https://doi.org/10.1016/j.scca.2025.100061.

[12] James R., A. M., C. Castorena, and W. Yuan. 2021. Modeling Product Distribution of Top-Lit Updraft Gasification. *BioResources*. 16(4): 6629–42. https://doi.org/10.15376/biores.16.4.6629-6642.

[13] Anderson, P. S., and S. J. S. Anderson. 2016. Origins, History, and Future of TLUD Micro-Gasification and Cookstove Advancement. *TLUD Technology*.

[14] Sánchez-Pólito, J., *et al*. 2024. Development and Evaluation Performance of Top-Lit Updraft Biomass Micro-Gasifiers for Energy-Intensive Household Cooking Tasks in Mexico. *Sustainable Energy Technologies and Assessments*. 103813. https://doi.org/10.1016/j.seta.2024.103813.

[15] Scharler, R., *et al.* 2021. Emission Minimization of a Top-Lit Updraft Gasifier Cookstove Based on Experiments and Detailed CFD Analyses. *Energy Conversion and Management*. 247: 114755. https://doi.org/10.1016/j.enconman.2021.114755.

[16] Minh Loy, A. C., *et al.* 2020. Optimization Study of Syngas Production from Catalytic Air Gasification of Rice Husk. *International Journal on Advanced Science, Engineering and Information Technology*. 10(5): 1784–91. https://doi.org/10.18517/ijaseit.10.5.9906.

[17] Shukla, S. S., R. Chava, S. Appari, B. A., and B. V. R. Kuncharam. 2022. Sustainable Use of Rice Husk for the Cleaner Production of Value-Added Products. *Journal of Environmental Chemical Engineering*. 10(1): 106899. https://doi.org/10.1016/j.jece.2021.106899.

[18] Corrêa, P. S. P., J. Zhang, E. E. S. Lora, R. V. Andrade, L. R. de Mello e Pinto, and A. Ratner. 2019. Experimental Study on Applying Biomass-Derived Syngas in a Microturbine. *Applied Thermal Engineering*. 146: 328–37. https://doi.org/10.1016/j.applthermaleng.2018.09.123.

[19] Ma, Y., W. Zheng, X. Guo, M. Tigabu, and F. Guo. 2021. Effect of Forest Floor Fuel Moisture Content on Chemical Components of $PM_{2.5}$ Emitted during Combustion. *Chemosphere*. 279: 130547. https://doi.org/10.1016/j.chemosphere.2021.130547.

[20] Romes, N. B., R. A. Wahab, and M. A. Hamid. 2019. Proximate Analysis and Bioactivity Study on Acoustically Isolated *Elaeis guineensis* Leaves Extract. *AIP Conference Proceedings*. American Institute of Physics. https://doi.org/10.1063/1.5125505.

[21] Maliki, M., E. U. Ikhuoria, and P. Aluyor. 2023. Proximate Analysis of Selected Agricultural Waste for Their Nutritional Potential. *North African Journal of Food and Nutrition*

Research. 7(15): 117–25. https://doi.org/10.51745/najfnr.7.15.117-125.

[22] Nguyen, N. M., F. Alobaid, P. Dieringer, and B. Epple. 2021. Biomass-Based Chemical Looping Gasification: Overview and Recent Developments. *Applied Sciences*. 11(15): 7069. https://doi.org/10.3390/app11157069.

[23] Steven, S., *et al.* 2022. Thermodynamics Simulation Performance of Rice Husk Combustion with a Realistic Decomposition Approach on the Devolatilization Stage. *Waste and Biomass Valorization*. 13(5): 2735–47. https://doi.org/10.1007/s12649-021-01657-x.

[24] Ahmad, R. K., S. A. Sulaiman, S. Yusup, S. S. Dol, M. Inayat, and H. A. Umar. 2022. Exploring the Potential of Coconut Shell Biomass for Charcoal Production. *Ain Shams Engineering Journal*. 13(1). https://doi.org/10.1016/j.asej.2021.05.013.

[25] Ríos-Badrán, I. M., I. Luzardo-Ocampo, J. F. García-Trejo, J. Santos-Cruz, and C. Gutiérrez-Antonio. 2020. Production and Characterization of Fuel Pellets from Rice Husk and Wheat Straw. *Renewable Energy*. 145: 500–507. https://doi.org/10.1016/j.renene.2019.06.048.

[26] Mehta, Y. 2018. Gasification and Combustion Studies in Top-Lit Updraft Gasifier Cookstove.

[27] Murad, E., and F. Dragomir. 2012. Heat Generators with TLUD Gasifier for Generating Energy from Biomass with a Negative Balance of CO_2.

[28] Hamad, M. A. F., A. M. Radwan, and A. Amin. 2017. Review of Biomass Thermal Gasification. *Biomass Volume Estimation and Valorization for Energy*. 488. https://doi.org/10.5772/66362

[29] James Rivas, Arthur M. 2015. Simultaneous Biochar and Syngas Production in a Top-Lit Updraft Biomass Gasifier. Accessed March 25, 2025. https://ridda2.utp.ac.pa/handle/123456789/5100.

[30] Quintero-Coronel, D. A., *et al.* 2023. Assessment of the Interchangeability of Coal–Biomass Syngas with Natural Gas for Atmospheric Burners and High-Pressure Combustion Applications. *Energy*. 276: 127551. https://doi.org/10.1016/j.energy.2023.127551.

[31] Shen, W., S. Wang, and X. Hou. 2023. Coupling Mechanism of Pressure and Temperature in a Co-Rotating Cavity with Radial Flow. *Thermal Science and Engineering Progress*. 43: 101940. https://doi.org/10.1016/j.tsep.2023.101940.

[32] Li, J., J. Liu, S. Liao, and R. Yan. 2010. Hydrogen-Rich Gas Production by Air–Steam Gasification of Rice Husk Using Supported Nano-NiO/γ-Al_2O_3 Catalyst. *International Journal of Hydrogen Energy*. 35(14): 7399–7404. https://doi.org/10.1016/j.ijhydene.2010.04.108.

[33] Saravanakumar, A., T. M. Haridasan, T. B. Reed, and R. K. Bai. 2007. Experimental Investigation and Modelling Study of Long Stick Wood Gasification in a Top-Lit Updraft Fixed-Bed Gasifier. *Fuel*. 86(17–18): 2846–56. https://doi.org/10.1016/j.fuel.2007.03.028.

[34] Patra, T. K., and P. N. Sheth. 2015. Biomass Gasification Models for Downdraft Gasifier: A State-of-the-Art Review. *Renewable and Sustainable Energy Reviews*. 50: 583–93. https://doi.org/10.1016/j.rser.2015.05.012.

[35] Dmitrenko, Y. M., and P. A. Klevan. 2011. Hydrogen Production in a Reversible Flow Filtration Combustion Reactor. *Journal of Engineering Physics and Thermophysics*. 84(6): 1296–1303. https://doi.org/10.1007/s10891-011-0597-2.

[36] Piyathissa, S. D. S., P. D. Kahandage, Namgay, H. Zhang, R. Noguchi, and T. Ahamed. 2023. Introducing a Novel Rice Husk Combustion Technology for Maximizing Energy and Amorphous Silica Production Using a Prototype Hybrid Rice Husk Burner to Minimize Environmental Impacts and Health Risk. *Energies*. 16(3): 1120. https://doi.org/10.3390/en16031120.

[37] Onthong, K., and J. Charoensuk. 2019. A New Method for Zone Development Observation for Updraft Rice Husk Gasification.

[38] Hendriyana, H. 2020. Effect of Equivalence Ratio on the Rice Husk Gasification Performance Using Updraft Gasifier with Air Suction Mode. *Jurnal Bahan Alam Terbarukan*. 9(1): 30–35. https://doi.org/10.15294/jbat.v9i1.23527.

[39] Serhan, M., *et al.* 2019. Total Iron Measurement in Human Serum with a Smartphone. Paper presented at the *AIChE Annual Meeting*. American Institute of Chemical Engineers.

[40] Eom, H., B. Jeon, and D. Shin. 2025. An Experimental Study on the Carbon Adsorption Performance of Biochar for Producing Carbon-Negative Turquoise Hydrogen. *International Journal of Hydrogen Energy*. 106: 1322–31. https://doi.org/10.1016/j.ijhydene.2025.01.093.